Biophysical Chemistry 253 (2019) 106217

Contents lists available at ScienceDirect

Biophysical Chemistry

journal homepage: www.elsevier.com/locate/biophyschem

Prediction of the size of electroformed giant unilamellar vesicle using response surface methodology

Salah Eddine Ghellab, Wei Mu, Qingchuang Li, Xiaojun Han*

State Key Laboratory of Urban Water Resource and Environment, School of Chemical Engineering and Technology, Harbin Institute of Technology, 92West Da-Zhi Street, Harbin 150001, China

HIGHLIGHTS

- Electroformation of GUVs at different potential, frequency and temperature.
- Prediction of GUVs diameter using response surface methodology.
- Understanding the influence of each parameter on GUVs size.
- Providing a 3D plot as guidance to produce suitable GUVs.

GRAPHICAL ABSTRACT

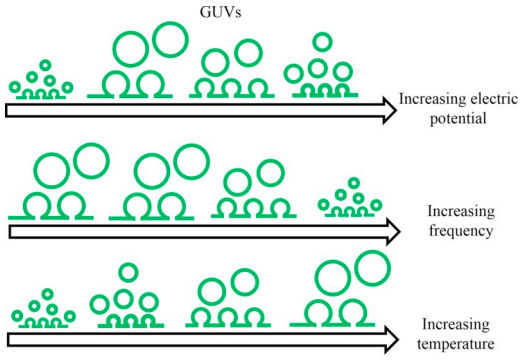

ARTICLE INFO

Keywords:
GUVs
Electroformation
Electric potential
Frequency
Temperature
Response surface methodology

ABSTRACT

The production of giant unilamellar vesicles (GUVs) with specific size and structure has been a challenge on the design of quantitative biological assays in cell-mimetic micro-compartments. In this study, the effect of electroformation parameters (electric potential, frequency, and temperature) on the size of GUVs was investigated. Using response surface methodology based on Box-Behnken design, GUVs from neutral, positive and negative charges were formulated. The average diameter of GUVs was determined for each formulation. The acquired data of these GUVs were successfully fitted with quadratic regression models. These models were applied to visualize the parameters for ideal GUVs with wanted diameters by the obtained phase diagrams. These results show that response surface methodology can be used to estimate the electroformation parameters for specifically sized GUVs.

1. Introduction

Giant unilamellar vesicles (GUVs) played important roles to study cell structures and functions due to their similarity with biological cells [1]. In last decades, an ever-increasing number of reports have focused on the GUVs. Their large diameter (Usually between 1 and 50 μm) makes them easy for the observation by a microscope. These cell-sized vesicles are widely used as membrane and cellular models [2], mimicking some biological phenomena such as cells deformation [3], cells adhesion [4], cells fusion [5], cells fission [6] and cells function studies [7]. GUVs encapsulating biologically active compounds have been used as drug delivery vehicles [8–10], platforms for synthetic biological systems [11], and microreactors [12,13]. Several preparation methods were carried out to form GUVs, such as hydration [14], emulsion

* Corresponding author.
E-mail address: hanxiaojun@hit.edu.cn (X. Han).

https://doi.org/10.1016/j.bpc.2019.106217
Received 29 March 2019; Received in revised form 1 July 2019; Accepted 1 July 2019
Available online 04 July 2019

transfer method [15], pulse jet method [16], and electroformation [17]. Electroformation technique is widely used for the formation of controllable GUVs with high yield, high unilamellarity, and few defect structure [18]. The method is based on the application of an AC electric voltage using two electrodes at given temperature [18–20].

The variation of the different parameters such as the applied electric voltage, frequency, and temperature, had significant influence on the size of the formed vesicles [18,21]. The investigation of the dependency of GUVs size on the electroformation parameters using a mathematical models capable to estimate the GUVs size will be beneficial for: 1) the selection of the optimum parameters in order to obtain the adequate size of GUVs for each application, 2) minimization of energy cost by choosing the minimum temperature and electric voltage, 3) minimizing the experiment runs in order to get the suitable size. Response Surface Methodology (RSM) is a collection of statistical and mathematical techniques to build empirical models [22,23]. This method is used to estimate, observe, and optimize a response (output) influenced by several independent variables (inputs) [24,25]. The optimum size for cell mimicking, GUVs with size higher than 12 μm is favorable in order to be visualized under fluorescence microscopy.

In this work, the effect of parameters (electric potential, frequency, and temperature) on GUV diameter was investigated using RSM. Quadratic polynomial equations are obtained to estimate the average size of GUVs from different lipids by the variation of the independent parameters of different lipids. The given model well matched the experimental measurements.

2. Materials

1,2-dioleoyl-sn-glycero-3-phosphocholine(DOPC), 1,2-dimyristoyl-sn-glycero-3-phosphocholine (DMPC), 1,2-dioleoyl-sn-glycero-3-phospholserine, sodium salt (DOPS), 1,2-dioleoyl-3-trimethylammonium-propane, chloride salt(DOTAP) were obtained from Avanti Polar Lipids (USA). Fluorescence-labeled1,2-dioleoyl-sn-glycero-3-phosphoethanolamine-N-(7-nitro-2 − 1,3 benzoxadiazol-4-yl) (NBD PE) was obtained from Invitrogen (China). Chloroform were purchased from Sigma (China). ITO electrodes (Indium tin oxide, sheet resistance ≈8–12 Ω, thickness ≈ 160 nm) were purchased from Hangzhou Yuhong technology Co. Ltd. (China). High purity Ethanol (> 99.5%) was purchased from FuYu Chemicals (China). Millipore Milli-Q water with a resistivity of 18.0 mΩ cm have been used for solution preparation in the electroformation experiment.

3. Experimental setups

The ITO electrodes (20 × 30 mm) were sonicated in water and ethanol for 15 min, dried by N_2, and plasma cleaned for 1 min. The flat-coating method is used to prepare a lipid thin films on the ITO electrodes [26]. Different lipids solution (DOPC /NBD PE and DMPC/NBD PE) with mass fraction of 98:2 and (DOTAP, DLPC, NBD PE, and DOPS, DLPC, NBD PE) with mass ratio 28:70:2 were dissolved in chloroform. The mass concentration of the prepared lipid was 5.0 mg/mL. For the preparation of lipid films, 5 μL of lipid solution was deposited on the glass surface by spreading carefully back and forth using a needle and dried under vacuum for 5 min. The coated glass slide was separated by a frame spacer with a thickness of 13 mm. The electroformation process was realized in distillated water for one hour. AC electric field is applied using a signal generator (TGA12104, England). The electroformed GUVs were observed under a fluorescence microscope (Nikon 80i, Japan). NIS element software was used for diameter measurement. The diameter was determined by fitting circles on randomly selected 300 GUVs. Each experiment was repeated 3 times, and for each measurement 300 GUVs were randomly selected, making sure that the squeezed GUVs were excluded from the diameter analysis. The effect of electric potential, frequency, and temperature on the lamellarity of GUVs and membrane defects was not considered in this study.

4. Results and discussion

4.1. Validation of electroformation of GUVs under different parameters

After drying the DOPC lipid film deposited on the ITO electrode surface for five minutes under vacuum, the electroformation chamber was gently filled with distilled water. An AC electric field was applied for one hour at different parameters. The vesicle diameters were measured. Another important characterization known as the polydispersity index (*PDI*) is the representation of the distribution of size populations within a given sample, which indicates the degree of non- uniformity of vesicles. The *PDI* of GUVs can be calculated by the eq. (1) [27]:

$$PDI = \left(\frac{\sigma}{D}\right)^2 \tag{1}$$

where D is the average diameter of GUVs and σ is the standard deviation. For perfect uniform sample, *PDI* is equal to 0. However, a value of 0.05 or below are mainly seen with highly mono disperse standard, meanwhile a value of 0.3 or below is considered to be acceptable and indicates a homogenous population of phospholipid vesicles [28].

As shown in Fig. 1, the electroformation of GUVs were formed for one hour at a fixed frequency (10 Hz), temperature (25 °C) and varied electric potential (1 V, 5 V, and 10 V) with the average diameter of 16.08 μm (1 V), 21.57 μm (5 V) and 17.48 μm (10 V) respectively. The *PDI* is 0.013, 0.052, and 0.048 respectively. The variation of vesicle size at different potentials confirms that the electric potential influences the size of GUVs.

To visualize the effect of frequency on the vesicles size, electroformation of GUVs for one hour at fixed electric potential (10 V), temperature (25 °C), and varied frequency (1 Hz, 10^2 Hz, 10^4 Hz) was carried out, as shown in Fig. 2. The average diameter was 18.45 μm, 17.34 μm and 8.88 μm respectively, the corresponding *PDI* is 0.028, 0.033, and 0.019 respectively. The average size dissimilarity confirms that the frequency influences on the GUVs size.

Another important parameter was also carried out. As shown in Fig. 3, electroformation of GUVs was also realized for one hour at a fixed electric potential (10 V), frequency (10 Hz), and varied temperature (25 °C, 35 °C, 45 °C) with the average size of the vesicles of 17.48 μm, 19.04 μm, and 23.01 μm respectively. The corresponding *PDI* is 0.023, 0.067 and 0.059 respectively. The dissimilarity of GUVs size shows the influence of temperature.

The electric voltage, frequency and temperature have an effect on the size of the formed GUVs. The size of GUVs has direct effect on their deformability, which means that the GUVs with bigger diameter has higher possibility to deform under flow, as shown in Fig. 3 a and 3c or Fig. 2a and c. These results are in accordance with Peterlin's [29]. He found a mathematical relationship between GUVs size and deformability.

In the following contexts, the influence of electric potential, frequency, and temperature on the size of GUVs will be visualized mathematically (Fig. 4).

4.2. Matrix design and models building

Three fundamental parameters (electric potential, frequency, and temperature) have an influence on the GUVs size. The maximum and the minimum level of each parameter for each lipid are determined experimentally. Inside this interval, the yield of GUVs was high, whilst outside the interval, no yield or low yield of vesicles was observed. The given parameters are accompanied with three-level Box Behnken design as shown in Table 1. In this work, Box Behnken design is developed for the estimation of response surfaces and constructs a second order polynomial model, which helps in the estimation and the prediction of GUVs size mathematically using a limited number of experimental runs. It is convenient to present the theoretical results in normalized units, so

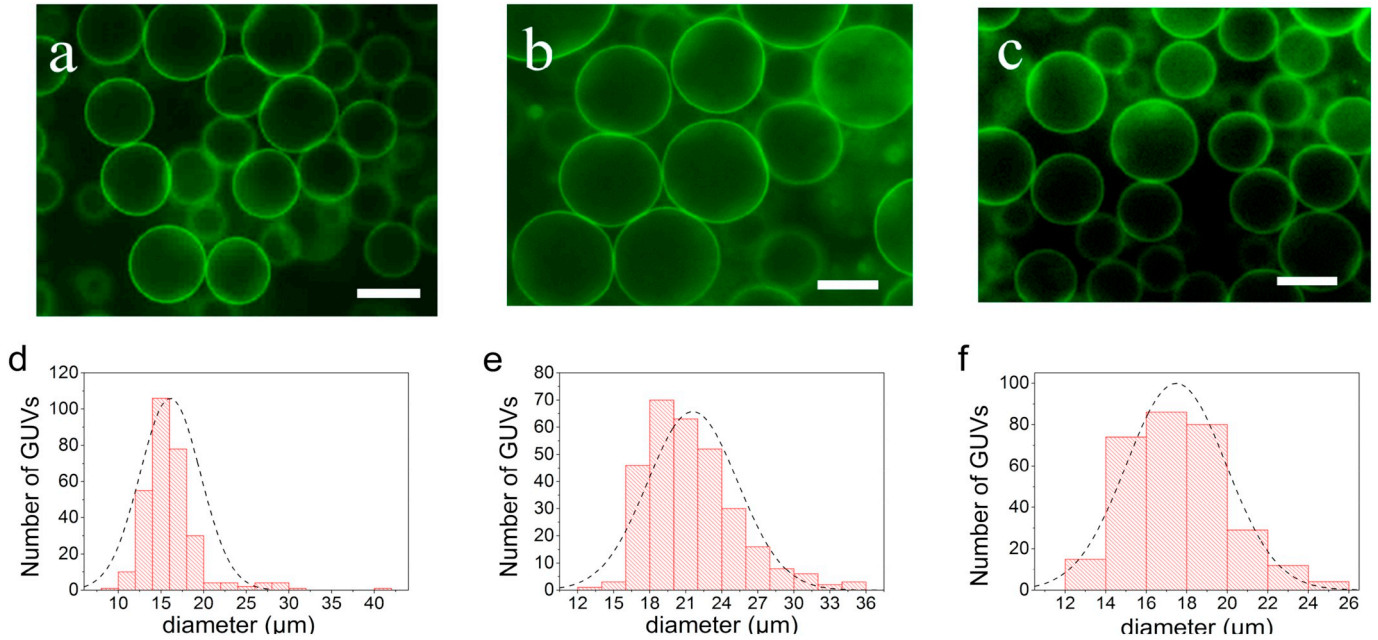

Fig. 1. DOPC GUVs formed by electroformation method. The temperature and frequency was fixed at 25 °C, and 10 Hz. The electric potential was: (a) = 1 V, (b) = 5 V, (c) = 10 V. The average diameter (D) was 16.08 μm, 22.67 μm, and 17.48 μm with *PDI* of 0.048, 0.032, and 0.019 respectively. (c), (d) and (f) are the histograms and size distribution of the GUVs given in a, b, and c respectively. For each experiment 300 GUVs were measured. The scale bars are 15 μm.

we define the variable x_1, x_2, x_3 and the response d as the normalized value of the electric potential (X_1), frequency (X_2), temperature (X_3), and the vesicles average diameter (D) respectively. They can be represented by the following Eqs. [23]:

$$x_i = \frac{X_i - X_{i0}}{\Delta X_i} \tag{2}$$

$$X_{i0} = \frac{X_{i\min} + X_{i\max}}{2} \tag{3}$$

$$\Delta X_i = \frac{X_{i\max} - X_{i\min}}{2} \tag{4}$$

$$d = \frac{D}{I} \tag{5}$$

where X_i is the given parameter at its real value, x_i is the normalized parameter, X_{i0}, $X_{i\max}$ and $X_{i\min}$ are the middle, the maximum and the minimum value of each parameter, I is the unit diameter and equal to 1 μ*m*. As a result, for each normalized parameter x_i, its value varies from −1 to 1.

The relation between the GUVs diameter and the given variables

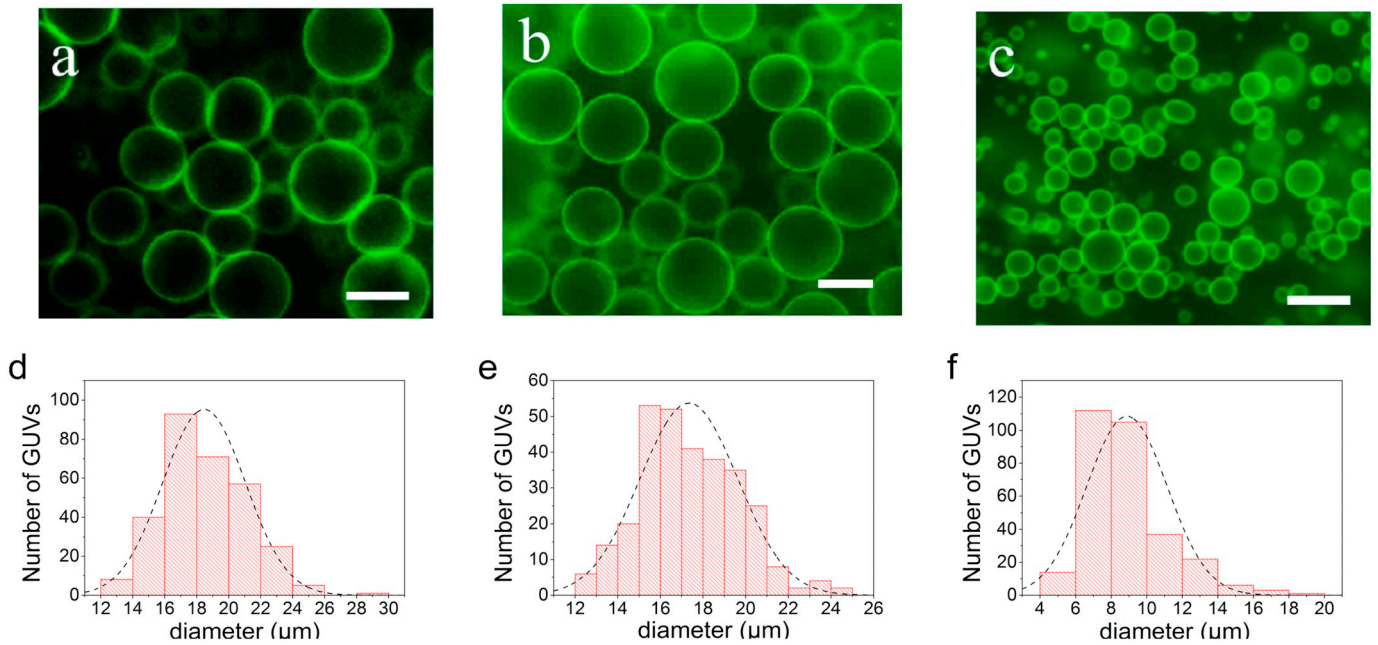

Fig. 2. DOPC GUVs formed by electroformation method. The amplitude and temperature was fixed at 10 V and 25 °C respectively. The frequency was: (a) = 1 Hz, (b) = 10^2 Hz, (c) = 10^4 Hz. The average diameter (D) was 18.45, 17.34, and 8.88with *PDI* of 0.029, 0.018, and 0.065 respectively. (c), (d) and (f) are the histograms and size distribution of the GUVs given in a, b, and c respectively. For each experiment 300 GUVs were measured. The scale bars are 15 μm.

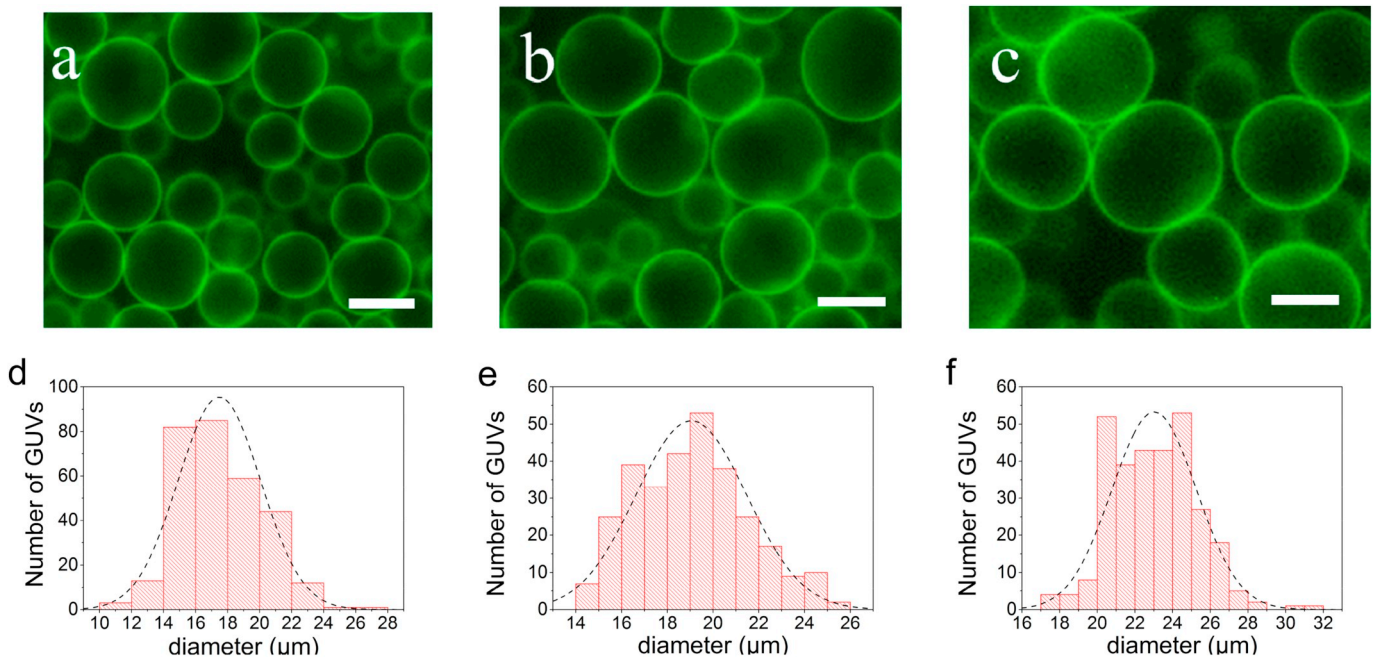

Fig. 3. DOPC GUVs formed by electroformation method, the amplitude and frequency was fixed at 10 V and 10 Hz respectively. The temperature was: (a) = 25 °C, (b) = 35 °C, (c) = 45 °C. The average diameter (D) was 17.48, 19.04, and 23.01 μm with *PDI* of 0.023, 0.016, and 0.039 respectively. (c), (d) and (f) are the histograms and size distribution of the GUVs given in a, b, and c respectively. For each experiment 300 GUVs were measured. The scale bars are 15 μm.

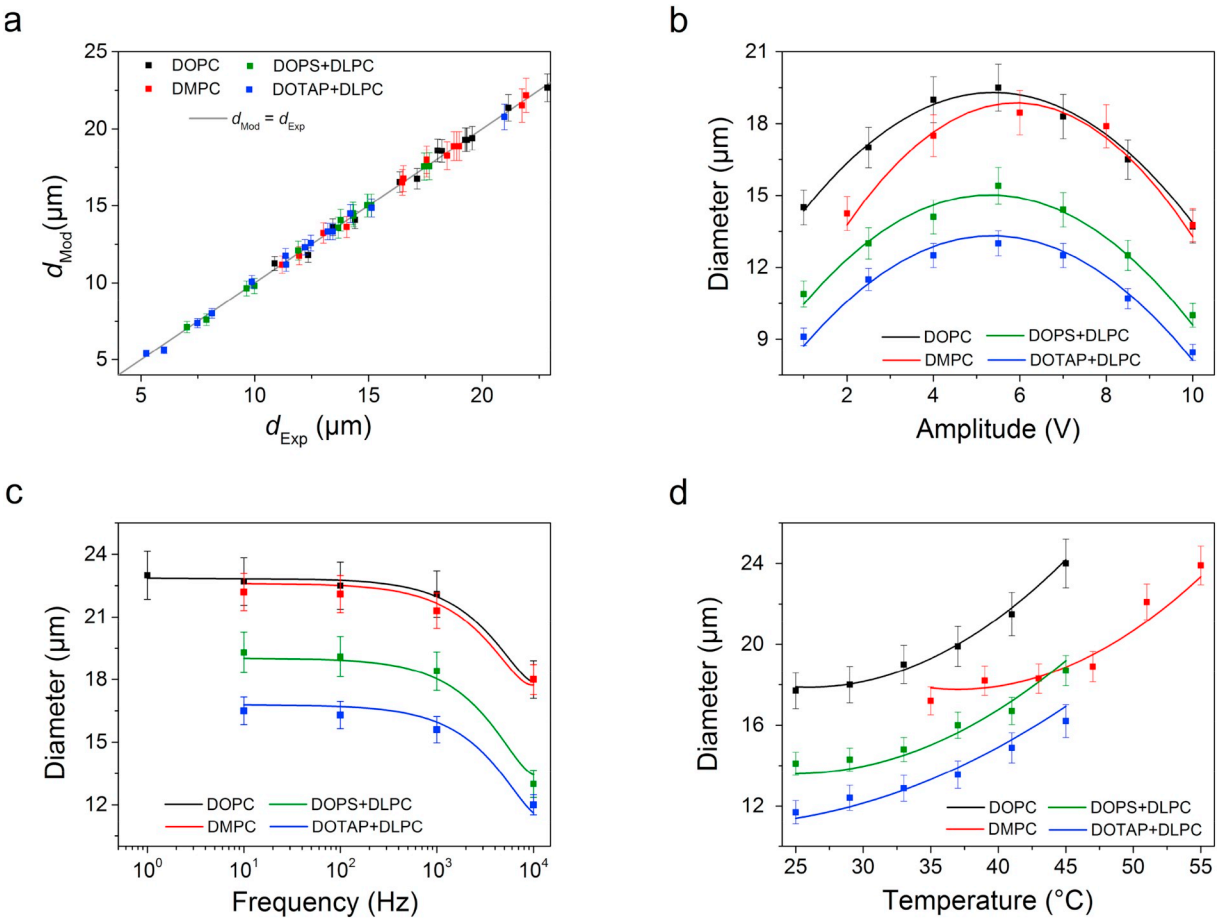

Fig. 4. (a) Comparison between experimental values given by Table 2 and the predicted values given by the models. (b) Variations of GUVs size as a function of electric potential with the frequency and temperature to be kept at the middle level for each lipid. (c) Variations of GUVs size as a function of frequency with the electric potential and temperature to be kept at the middle level for each lipid. (d) Variations of GUVs size as a function of temperature with the electric potential and frequency to be kept at the middle level. The continuous lines are obtained from the proposed models, while the dots were the experimental data.

Table 1
Range and levels of the independent parameters X_1, X_2 and X_3 for each lipid.

Variable	Lowest value (X_{imin})				Middle value (X_{i0})				Highest value (X_{imax})			
	DOPC	DMPC	DOPS + DLPC	DOTAP + DLPC	DOPC	DMPC	DOPS + DLPC	DOTAP + DLPC	DOPC	DMPC	DOPS + DLPC	DOTAP + DLPC
X_1 (V)	1	2	1	1	5.5	6	5.5	5.5	10	10	10	10
X_2 (Hz)	1	10	10	10	5000.5	5005	5005	5005	10^4	10^4	10^4	10^4
X_3 ($^\circ C$)	25	35	25	25	35	45	35	35	45	55	45	45

can be expressed by the following Eq. [23]:

$$d = a_0 + \sum_{i=1}^{k} a_i x_i + \left\{ \sum_{i=1}^{k-1} \sum_{j=i+1}^{k} a_{ij} x_i x_j \right\} + \sum_{i=1}^{k} a_{ii} x_i^2 + \varepsilon \quad (5)$$

where, k is the number of variables, for 3 independent variable $k = 3$, a_0 is the constant effect, a_1, a_2, and a_3 is the linear effect, a_{ij}, is the interaction effect between the parameters, a_{ii} is the quadratic effect. ε is the error between the real and the estimated diameter. For three independent variables, the eq. (5) could be simplified to be:

$$d = a_0 + a_1x_1 + a_2x_2 + a_3x_3 + a_{12}x_1x_2 + a_{13}x_1x_3 + a_{23}x_2x_3 + a_{11}x_1^2 + a_{22}x_2^2 + a_{33}x_3^2 \quad (6)$$

The model's effects a_i, a_{ij}, and a_{ii} are calculated from the eq. (7):

$$A = (X^tX)^{-1}X^tD \quad (7)$$

where A is the effect matrix, X is the associated model matrix, and X^t is transposed of the associated model matrix, D is the output matrix, the definition of A, X, and D is given in the supporting information.

To calculate the effects, a multiple regression analysis is performed, which can be used to predict the response (d). The operating conditions of amplitude, frequency and temperature using different lipids, are regrouped in Table 2 showing their normalized values.

The results in Table 2 confirm an effective electroformation of GUVs from different lipids at different conditions of electric potential, frequency, and temperature. Moreover, the *PDI* was smaller than 0.1, which indicate the good homogeneity of the formed vesicles.

In this work, the response surface methodology was carried out to evaluate the different effects of the three main independent parameters (electric potential, frequency, and temperature) on the size of GUVs. Based on the results obtained in Table 2, an empirical relationship between the vesicles diameter and the independent parameters was obtained. The following quadratic polynomial equations for each lipid solution are reflected in Table 3:

We note that the obtained models are valid only for the same materials and experimental conditions mentioned in the Section 2, and any change in the electrolyte composition, lipid type, ITO coating resistance or electrode distance can also effect on the size of GUVs.

4.3. Models validation

The analysis of variance (ANOVA) of the empiric quadratic models is reflected in Table 4. To assure the reliability of the obtained models, the correlation factor R^2 for each model was expressed by plotting the predicted responses cross the observed ones as shown in Fig. 4a. The estimated value of R^2 was 0.985, 0.981, 0.994 and 0.991 for DOPC, DMPC, DLPC + DOPS, and DLPC + DOTAP models respectively, which indicates a good agreement between the experiment and the predicted values. The adjusted R^2 (Adj-R^2) was also calculated for correction of the determination coefficient R^2. It was found to be 0.982, 0.976, 0.986 and 0.982 for DOPC, DMPC, DLPC + DOPS, and DLPC + DOTAP models respectively, which was in accordance with R^2 value. The Fisher variation ratio F-value is defined as the ratio between the mean square of the model and the residual error. It indicates how well the factors describe the data variation around its mean [30]. If the model gives a good prediction of the experimental results, the F-value must be greater than the critical value Fc at a given level of significance α (α = 5%). In our case F-value was 194.19, 117.33, 433.49, and 209.94 which was greater than the critical value Fc (Fc = 4.77 [25]), this confirms that the quadratic models were very adequate and significant.

4.4. Effect of individual parameters on the formation of GUVs

The effect of electric potential on the GUVs size is reflected in Fig. 4b. For low electric potential (< 6 V), the vesicle diameter increases with increasing of the electric potential, which could be explained by the increase of the electroosmotic flow related to the electric field [31]. However, for high electric potential (> 6 V), the vesicle diameter decreases with increasing of electric potential. It could be explained by the oxidation of lipid molecules which lead to the rupture of the lipid bilayer and the formation of small GUVs [32].

The effect of frequency is reflected in Fig. 4c. At low frequency (< 10^3 Hz) the vesicles size didn't have an important variation. However, at high frequency (> 10^3 Hz), the vesicle size decreases with

Table 2
Box-Behnken Matrix design in normalized units along with the measured responses.

Experimental run	x_1	x_2	x_3	DOPC		DMPC		DOPS + DLPC		DOTAP + DLPC	
				d	*PDI*	*d*	*PDI*	*d*	*PDI*	*d*	*PDI*
1	−1	−1	0	17.14	0.044	16.49	0.028	13.67	0.039	11.38	0.022
2	1	−1	0	18.23	0.036	17.56	0.041	14.32	0.045	12.47	0.036
3	−1	1	0	14.41	0.048	14.04	0.034	9.98	0.052	8.12	0.054
4	1	1	0	10.87	0.035	11.21	0.038	7.02	0.062	5.23	0.042
5	−1	0	−1	13.43	0.055	13.02	0.029	9.64	0.036	7.48	0.032
6	1	0	−1	12.35	0.027	11.95	0.041	7.88	0.043	6.01	0.051
7	−1	0	1	18.04	0.056	17.56	0.049	13.78	0.055	11.36	0.083
8	1	0	1	19.56	0.047	18.46	0.055	14.34	0.078	12.21	0.046
9	0	−1	−1	21.15	0.065	21.75	0.078	17.45	0.088	14.20	0.069
10	0	1	−1	16.37	0.036	16.54	0.043	11.91	0.063	9.87	0.072
11	0	-1	1	28.01	0.068	27.36	0.062	23.42	0.056	20.98	0.041
12	0	1	1	22.87	0.051	21.93	0.055	17.67	0.048	15.14	0.055
13	0	0	0	19.33	0.044	16.98	0.038	15.12	0.056	13.43	0.037

Table 3
the quadratic models predicting the variation of GUVs diameter, as a function of normalized parameters.

Lipid	Quadratic model
DOPC	$d = 19.2933 - 0.2513x_1 - 2.5006x_2 + 3.1469x_3 - 1.1575x_1x_2 + 0.6500x_2x_3 - 0.0913x_1x_3 - 5.1935x_1^2 + 1.0627x_2^2 + 1.7452x_3^2$
DMPC	$d = 18.87 - 0.2412x_1 - 2.4306x_2 + 2.7563x_3 - 0.975x_1x_2 + 0.4929x_2x_3 - 0.055x_1x_3 - 5.3462x_1^2 + 1.313x_2^2 + 1.7238x_3^2$
DOPS + DLPC	$d = 15.0167 - 0.4388x_1 - 2.7850x_2 + 2.7913x_3 - 0.9025x_1x_2 + 0.5800x_2x_3 - 0.0525x_1x_3 - 4.9858x_1^2 + 1.2167x_2^2 + 1.3792x_3^2$
DOTAP + DLPC	$d = 13.3167 - 0.3025x_1 - 2.5838x_2 + 2.6763x_3 - 0.9950x_1x_2 + 0.5800x_2x_3 - 0.3775x_1x_3 - 4.8996x_1^2 + 0.8829x_2^2 + 0.8479x_3^2$

Table 4
Analysis of variance (ANOVA) of the quadratic models based on Box-Behnken design.

Lipid model	F-value	Fc	Adj-R^2
DOPC	194.19	4.77 [25]	0.982
DMPC	117.33		0.976
DLPC + DOPS	433.49		0.986
DLPC + DOTAP	209.94		0.982

increasing of frequency. This observation was in accordance with others [33]. the size decrease can be explained by the decrease of the pulling force which decreases at high frequencies [34].

The effect of temperature on the diameters of GUVs is reflected in Fig. 4d. The GUVs diameter increases with increasing of temperature. It can be explained by the decreasing of the bending modulus which increase the fluidity during the electroformation process [35].

For each given parameters, the size of GUVs differs from one lipid to other. The size of DOPC GUVs was the biggest, followed by DMPC, DOPS + DLPC, and DOTAP + DLPC GUVs. This size difference may be explained by the different transition temperature of each lipid. A lower phase transition temperature may help the bilayer to separate and bend. This observation was in accordance with our previous result [19]. The RSM leads to contour plots in order to investigate the GUVs diameters varied with two factors and keeping the third at its central level, as shown in Fig. 5.

Fig. 5a shows the phase diagram of electric potential (x_1)-frequency (x_2) for a fixed temperature of 35 °C. The biggest GUVs size observed was at low frequency and middle amplitude (d ≈ 30 μm). Whereas the minimum diameter was obtained at low or high values of amplitude and high frequency (d ≈ 11 μm).

The Fig. 5b illustrates the phase diagram of frequency (x_2) and temperature (x_3) at a fixed electric potential (5.5 V). It indicates the high level of temperature accompanied with a low level of frequency allowed the formation of GUVs with a diameter no < 27 μm. By decreasing the temperature and increasing the frequency, the GUVs

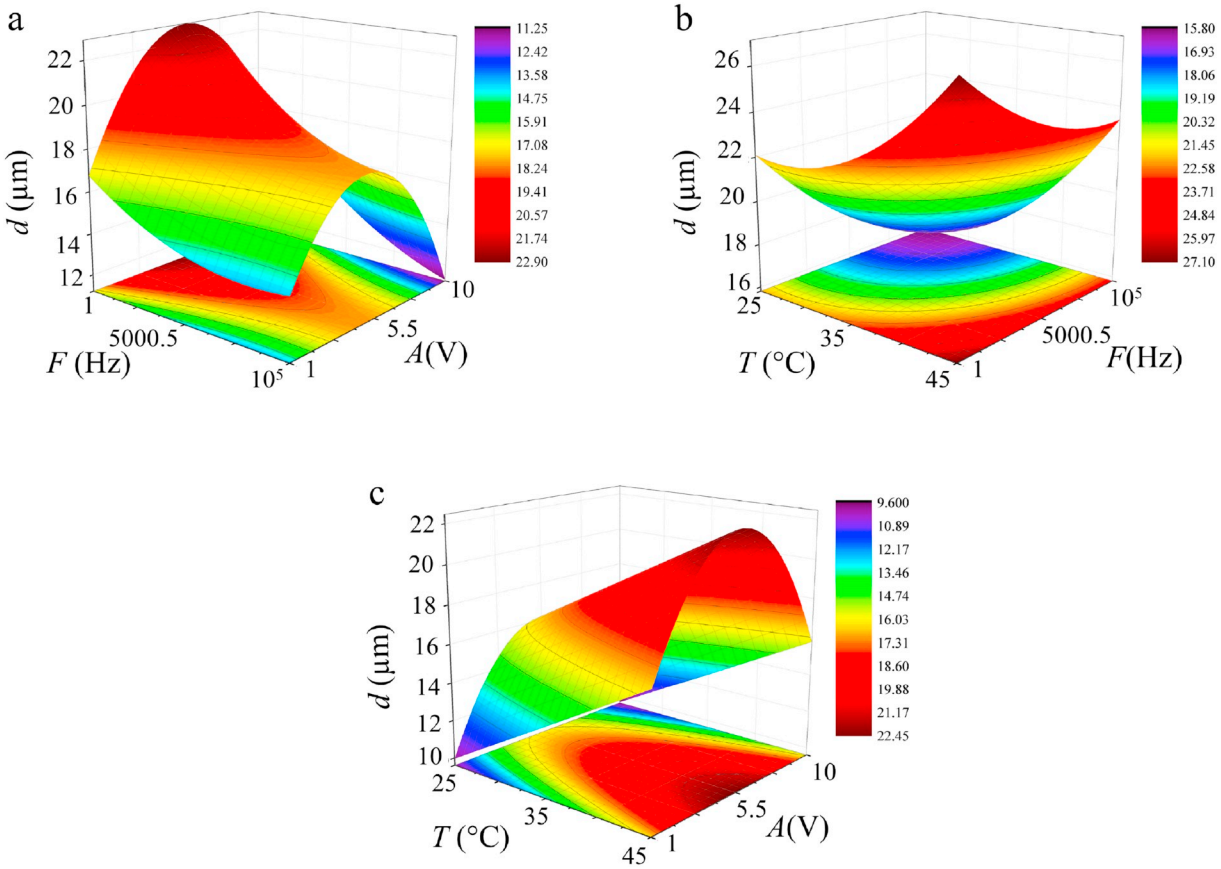

Fig. 5. 3D plots with projections of the DOPC GUVs size influenced by varying two of parameters (electric potential, frequency and Temperature) while keeping a fixed temperature (T = 35 °C; x_3 = 0.) (a), fixed electric potential (A = 5.5 V; x_1 = 0) (b), and fixed frequency (F = 5000.5 Hz; x_2 = 0) (c).

diameter could be decreased to < 15 μm.

The Fig. 5c represents the phase diagram of the electric potential and temperature at a fixed frequency. For minimum temperature, the minimum diameter of GUVs was found at low and high electric potential regions (< 10 μm). For maximum temperature, a maximum diameter (around 22 μm) was observed approaching to the central value of electric potential (5.5 V).

5. Conclusion

In this paper, electroformation method was performed for the formation of GUVs using an AC electric field. GUVs with different size have been obtained using different parameters of electric potential, frequency, and temperature. To estimate the size dependency of GUVs at different parameters, a quadratic regression was performed for different lipids. These models are based on Box-Behnken of RSM. A quadratic polynomial has been successfully used to estimate the diameter of the formed GUVs. The validations of models were confirmed by the high correlation coefficients R^2 and estimated adjusted adj-R^2. The obtained 3D plots are the guidance on the parameters to produce the suitable GUVs.

Acknowledgment

This work was supported by the National Natural Science Foundation of China (Grant No. 21773050), the Natural Science Foundation of Heilongjiang Province for Distinguished Young Scholars (JC2018003).

Appendix A. Supplementary data

Supplementary data to this article can be found online at https://doi.org/10.1016/j.bpc.2019.106217.

References

[1] E. Rideau, R. Dimova, P. Schwille, F.R. Wurm, K. Landfester, Liposomes and polymersomes: a comparative review towards cell mimicking, Chem. Soc. Rev. 47 (2018) 8572–8610.
[2] S. Deshpande, W.K. Spoelstra, M. van Doorn, J. Kerssemakers, C. Dekker, Mechanical division of cell-sized liposomes, ACS Nano 12 (3) (2018) 2560–2568.
[3] W. Zong, Q. Li, X. Zhang, X. Han, Deformation of giant unilamellar vesicles under osmotic stress, Colloids Surf. B: Biointerfaces 172 (2018) 459–463.
[4] S. Villringer, J. Madl, T. Sych, C. Manner, A. Imberty, W. Römer, Lectin-mediated protocell crosslinking to mimic cell-cell junctions and adhesion, Sci. Rep. 8 (1) (2018) 1932.
[5] R. Worch, J. Krupa, A. Filipek, A. Szymaniec, P. Setny, Three conserved C-terminal residues of influenza fusion peptide alter its behavior at the membrane interface, Biochim. Biophys. Acta (BBA)-General Subj. 1861 (2) (2017) 97–105.
[6] W. Zong, S. Ma, X. Zhang, X. Wang, Q. Li, X. Han, A fissionable artificial eukaryote-like cell model, J. Am. Chem. Soc. 139 (29) (2017) 9955–9960.
[7] C. Zhu, Q. Li, M. Dong, X. Han, Giant Unilamellar vesicle microarrays for cell function study, Anal. Chem. 90 (24) (2018) 14363–14367.
[8] X. Zhang, W. Zong, H. Bi, K. Zhao, T. Fuhs, Y. Hu, W. Cheng, X. Han, Hierarchical drug release of pH-sensitive liposomes encapsulating aqueous two phase system, Eur. J. Pharm. Biopharm. 127 (2018) 177–182.
[9] N. Wilkosz, S. Rissanen, M. Cyza, R. Szybka, M. Nowakowska, A. Bunker, T. Róg, M. Kepczynski, Effect of piroxicam on lipid membranes: drug encapsulation and gastric toxicity aspects, Eur. J. Pharm. Sci. 100 (2017) 116–125.
[10] W. Zong, Y. Hu, Y. Su, N. Luo, X. Zhang, Q. Li, X. Han, Polydopamine-coated liposomes as pH-sensitive anticancer drug carriers, J. Microencapsul. 33 (3) (2016) 257–262.
[11] M. Garni, T. Einfalt, R. Goers, C.G. Palivan, W.P. Meier, Live follow-up of enzymatic reactions inside the cavities of synthetic giant unilamellar vesicles (GUVs) equipped with membrane proteins mimicking cell architecture, ACS Synth. Biol. 7 (9) (2018) 2116–2125.
[12] C. Zhu, F. Itel, R. Chandrawati, X. Han, B. Städler, Multi-compartmentalized microreactors containing nuclei and catalase-loaded liposomes, Biomacromolecules 19 (11) (2018) 4379–4385.
[13] Y. Elani, R.V. Law, O. Ces, Vesicle-based artificial cells as chemical microreactors with spatially segregated reaction pathways, Nat. Commun. 5 (2014) 5305.
[14] K.S. Horger, D.J. Estes, R. Capone, M. Mayer, Films of agarose enable rapid formation of giant liposomes in solutions of physiologic ionic strength, J. Am. Chem. Soc. 131 (5) (2009) 1810–1819.
[15] G. Tsuji, T. Sunami, N. Ichihashi, Production of giant unilamellar vesicles by the water-in-oil emulsion-transfer method without high internal concentrations of sugars, J. Biosci. Bioeng. 126 (4) (2018) 540–545.
[16] D.L. Richmond, E.M. Schmid, S. Martens, J.C. Stachowiak, N. Liska, D.A. Fletcher, Forming giant vesicles with controlled membrane composition, asymmetry, and contents, Proc. Natl. Acad. Sci. 108 (23) (2011) 9431–9436.
[17] M. Le Berre, A. Yamada, L. Reck, Y. Chen, D. Baigl, Electroformation of giant phospholipid vesicles on a silicon substrate: advantages of controllable surface properties, Langmuir 24 (6) (2008) 2643–2649.
[18] Y.P. Patil, S. Jadhav, Novel methods for liposome preparation, Chem. Phys. Lipids 177 (2014) 8–18.
[19] Q. Li, X. Wang, S. Ma, Y. Zhang, X. Han, Electroformation of giant unilamellar vesicles in saline solution, Colloids Surf. B: Biointerfaces 147 (2016) 368–375.
[20] H. Bi, D. Fu, L. Wang, X. Han, Lipid nanotube formation using space-regulated electric field above interdigitated electrodes, ACS Nano 8 (4) (2014) 3961–3969.
[21] P. Taylor, C. Xu, P.D. Fletcher, V.N. Paunov, A novel technique for preparation of monodisperse giant liposomes, Chem. Commun. (14) (2003) 1732–1733.
[22] R.H. Myers, D.C. Montgomery, Response Surface Methodology: Process and Product Optimization Using Designed Experiments, vol. 4, Wiley, New York, 1995.
[23] M.A. Bezerra, R.E. Santelli, E.P. Oliveira, L.S. Villar, L.A. Escaleira, Response surface methodology (RSM) as a tool for optimization in analytical chemistry, Talanta 76 (5) (2008) 965–977.
[24] P.C. Soema, G.-J. Willems, W. Jiskoot, J.-P. Amorij, G.F. Kersten, Predicting the influence of liposomal lipid composition on liposome size, zeta potential and liposome-induced dendritic cell maturation using a design of experiments approach, Eur. J. Pharm. Biopharm. 94 (2015) 427–435.
[25] A. Belbaki, W. Louaer, A.-H. Meniai, Supercritical CO2 extraction of oil from crushed Algerian olives, J. Supercrit. Fluids 130 (2017) 165–171.
[26] C. Herold, G. Chwastek, P. Schwille, E.P. Petrov, Efficient electroformation of supergiant unilamellar vesicles containing cationic lipids on ITO-coated electrodes, Langmuir 28 (13) (2012) 5518–5521.
[27] N. Kozlov, U. Natashina, K. Tamarov, M. Gongalsky, V. Solovyev, A. Kudryavtsev, V. Sivakov, L. Osminkina, Recycling of silicon: from industrial waste to biocompatible nanoparticles for nanomedicine, Mater. Res. Expr. 4 (9) (2017) 095026.
[28] M. Danaei, M. Dehghankhold, S. Ataei, F. Hasanzadeh Davarani, R. Javanmard, A. Dokhani, S. Khorasani, M. Mozafari, Impact of particle size and polydispersity index on the clinical applications of lipidic nanocarrier systems, Pharmaceutics 10 (2) (2018) 57.
[29] P. Peterlin, Frequency-dependent electrodeformation of giant phospholipid vesicles in AC electric field, J. Biol. Phys. 36 (4) (2010) 339–354.
[30] R.H. Myers, R.H. Myers, Classical and Modern Regression with Applications, vol. 2, Duxbury Press, Belmont, CA, 1990.
[31] S.E. Ghellab, X. Han, Lipid tubes formation induced by electroosmotic flow, Chem. Phys. Lett. 706 (2018) 515–519.
[32] M. Breton, M. Amirkavei, L.M. Mir, Optimization of the electroformation of giant unilamellar vesicles (GUVs) with unsaturated phospholipids, J. Membr. Biol. 248 (5) (2015) 827–835.
[33] T.J. Politano, V.E. Froude, B. Jing, Y. Zhu, AC-electric field dependent electroformation of giant lipid vesicles, Colloids Surf. B: Biointerfaces 79 (1) (2010) 75–82.
[34] S.E. Ghellab, Q. Li, T. Fuhs, H. Bi, X. Han, Electroformation of double vesicles using an amplitude modulated electric field, Colloids Surf. B: Biointerfaces 160 (2017) 697–703.
[35] T. Shimanouchi, H. Umakoshi, R. Kuboi, Kinetic study on giant vesicle formation with electroformation method, Langmuir 25 (9) (2009) 4835–4840.